Physics Letters B 749 (2015) 215–220

Contents lists available at ScienceDirect

Physics Letters B

www.elsevier.com/locate/physletb

Parameterization of deformed nuclei for Glauber modeling in relativistic heavy ion collisions

Q.Y. Shou [a,b,*], Y.G. Ma [a], P. Sorensen [c], A.H. Tang [c], F. Videbæk [c], H. Wang [c]

[a] Shanghai Institute of Applied Physics, Chinese Academy of Sciences, Shanghai 201800, China
[b] Key Laboratory of Quark and Lepton Physics (MOE) and Institute of Particle Physics, Central China Normal University, Wuhan 430079, China
[c] Brookhaven National Laboratory, Upton, NY 11973, USA

ARTICLE INFO

Article history:
Received 26 March 2015
Received in revised form 30 July 2015
Accepted 30 July 2015
Available online 4 August 2015
Editor: V. Metag

ABSTRACT

The density distributions of large nuclei are typically modeled with a Woods–Saxon distribution characterized by a radius R_0 and skin depth a. Deformation parameters β are then introduced to describe non-spherical nuclei using an expansion in spherical harmonics $R_0(1+\beta_2 Y_2^0+\beta_4 Y_4^0)$. But when a nucleus is non-spherical, the R_0 and a inferred from electron scattering experiments that integrate over all nuclear orientations cannot be used directly as the parameters in the Woods–Saxon distribution. In addition, the β_2 values typically derived from the reduced electric quadrupole transition probability B(E2)↑ are not directly related to the β_2 values used in the spherical harmonic expansion. B(E2)↑ is more accurately related to the intrinsic quadrupole moment Q_0 than to β_2. One can however calculate Q_0 for a given β_2 and then derive B(E2)↑ from Q_0. In this paper we calculate and tabulate the R_0, a, and β_2 values that when used in a Woods–Saxon distribution, will give results consistent with electron scattering data. We then present calculations of the second and third harmonic participant eccentricity (ε_2 and ε_3) with the new and old parameters. We demonstrate that ε_3 is particularly sensitive to a and argue that using the incorrect value of a has important implications for the extraction of viscosity to entropy ratio (η/s) from the QGP created in Heavy Ion collisions.

1. Introduction

In relativistic nucleus–nucleus collisions, the geometry of the initial overlap region is reflected in the final momentum space distributions of produced particles [1–3]. How much that geometry is translated into the final state distributions is used to infer information about the properties of the matter created in the collision fireball like its viscosity [4]. The initial geometry plays a particularly important role in interpreting the data and in extracting the viscosity to entropy ratio η/s. It is important therefore to understand the initial conditions including the exact shape of the colliding nuclei. The inference of the properties of the fireball from data is hindered by uncertainties in the characteristics of the initial state [5]. Recently collisions between Uranium nuclei (^{238}U) which have an intrinsic prolate shape [6], have been used as a way to manipulate this initial geometry in order better test our understanding of the initial state of heavy ion collisions and the subsequent fireball [7,8].

An important part of describing the initial conditions is to correctly model the geometry of the incoming nuclei. For many years in simulations for heavy ion collisions, nuclei were approximated as smooth density distributions and the only anisotropies considered in the initial state were the intrinsic almond shape caused by the overlap of two spherical nuclei. As the accumulation of RHIC data gradually demonstrated that final state anisotropies were sensitive to the initial geometry and its fluctuations, it became necessary to take into account the lumpiness of the colliding nuclei [9–14]. This is done through Monte-Carlo simulations (M-C) where each nucleus is generated with a finite number of nucleons distributed with a density ρ described by a Woods–Saxon distribution [15]:

$$\rho(r) = \frac{\rho_0}{1+e^{(r-R_0)/a}}, \tag{1}$$

where ρ_0 is the density at the center of the nucleus. The nuclear radius R_0 and skin depth a are commonly taken from high-energy electron scattering measurements [16]. For non-spherical nuclei, this description was extended by introducing spherical harmonics in the Woods–Saxon distribution to describe the modulation of

* Corresponding author.
E-mail address: qiye.shou@cern.ch (Q.Y. Shou).

http://dx.doi.org/10.1016/j.physletb.2015.07.078

the nuclear radius with θ [17]:

$$\rho(r,\theta) = \frac{\rho_0}{1+e^{(r-R_0-R_0\beta_2 Y_{20}(\theta)-R_0\beta_4 Y_{40}(\theta))/a}}, \tag{2}$$

where β_2 and β_4 are the deformation parameters. β_2 is often derived from measurements of the reduced electric quadrupole transition probability B(E2)↑ from the 0^+ ground state to the first 2^+ state [6] according to the formula:

$$\beta_2 = \frac{4\pi}{3ZR_0^2}\sqrt{\frac{\mathrm{B(E2)}\uparrow}{e^2}}. \tag{3}$$

R_0 is taken to be $1.2A^{1/3}$. The B(E2)↑ values are directly measured experimental quantities, but the derivation of β_2 from B(E2)↑ is usually done with model dependent assumptions including the assumption that the nuclear charge distribution is a hard edged, step-function rather than a Woods–Saxon distribution. In order to check for consistency with the measured B(E2)↑ values, one can vary the β_2 used in Eq. (2) and then calculate the intrinsic quadrupole moment of the resulting nucleus:

$$Q_{20} = \sqrt{\frac{16\pi}{5}}\int d^3r\langle\Psi|r^2Y_{20}\rho(\vec{r})|\Psi\rangle \tag{4}$$

and check to ensure that Q_{20} is consistent with the measured B(E2)↑ according to the approximation [18]:

$$\mathrm{B(E2)}\uparrow = \frac{5}{16\pi}|eQ_{20}|^2. \tag{5}$$

This procedure ensures that the deformation of the simulated nucleus is consistent with the measured B(E2)↑ values for the given model describing the density profile of the nucleus.

Another difficulty in characterizing deformed nuclei comes from a mismatch between the parameters inferred from electron scattering experiments and the Woods–Saxon parameters used in the simulation of the nuclear density profile. Electron scattering experiments probe the spherical part of the density distribution (characterized by radius R_0 and diffuseness a), which is averaged over all orientations of the nucleus. If the nucleus is not spherical, then the R_0 and a used in Eq. (2) will not necessarily correspond to the average radius and average diffuseness inferred from the electron scattering experiments [16]. For this reason, it is important to calculate the R_0, a, and β_2 values that when used in conjunction with Eq. (2) yield a nucleus that is consistent with the experimental measurements of B(E2)↑, R_0 and a. In this paper we present updated R_0 and a for nuclei commonly used in collisions at RHIC or the LHC, ^{238}U, ^{208}Pb and ^{197}Au, as well as β_2 value for ^{238}U. We then show calculations of the second and third harmonic participant eccentricity ε_2 and ε_3 for the new and old parameters. We find that in addition to the obvious dependence of ε_2 on β_2, the ratio of $\varepsilon_3/\varepsilon_2$ is very sensitive to the diffuseness parameter a: ε_3 increases with increasing a while ε_2 decreases so that $\varepsilon_3/\varepsilon_2$ is overestimated if a is overestimated. Since viscous damping decreases the ratio of triangular flow over elliptic flow (v_3/v_2), an overestimate of $\varepsilon_3/\varepsilon_2$ will lead to an over-estimate of the amount of viscous damping needed to match the experimental data. We find therefore that the new values of a presented in this work should lead to a decrease in the value of η/s inferred from model-to-data comparisons.

2. Parameterization of deformed nuclei

When using a Woods–Saxon distribution with parameters R_0, a, and β_2 to characterize the density distribution of a deformed nucleus, it is obvious that after allowing for all possible rotations

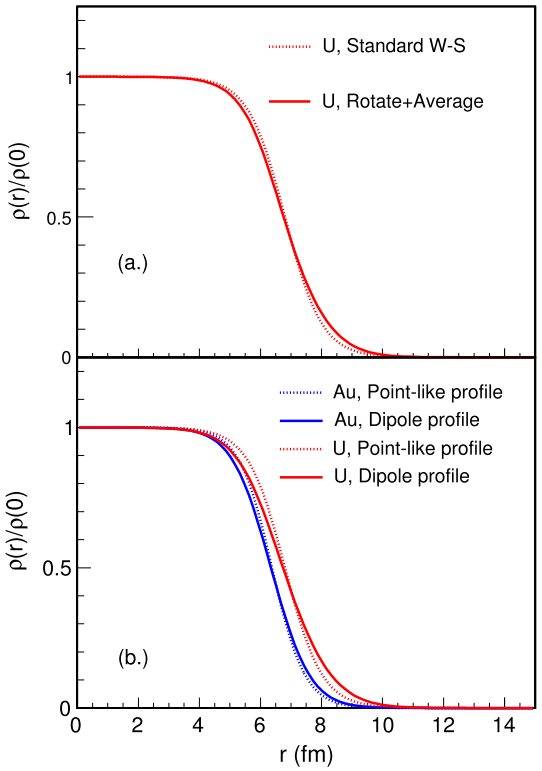

Fig. 1. (a) The nucleon density of a deformed nucleus U as a function of the radius can be recovered rotating and averaging. (b) Comparison of the nuclear charge density between different nuclei and nucleonic profiles. (For interpretation of the references to color in this figure legend, the reader is referred to the web version of this article.)

of the nucleus, the averaged density distribution will still be accurately described by a Woods–Saxon distribution. We find however, that for the range of R_0, a, and β_2 values describing typical nuclei, the final density distribution after averaging over all appropriate rotations is indeed well described by a Woods–Saxon distribution but with a different radius R_0' and diffuseness a'. To accurately model a nucleus, R_0' and a' should match the parameters measured in electron scattering experiments. The larger β_2 is, however, the more R_0' and a' deviate from the R_0 and a used in Eq. (2).

Taking $\rho(r,\theta)$ to be the density distribution of a deformed nucleus centered at the origin of the spherical coordinate system, then with n-times randomly rotated and overlapping ellipsoids, the total nucleon number of these n ellipsoids reads:

$$n\iiint \rho(r,\theta)r^2 sin(\theta)\,dr\,d\theta\,d\phi. \tag{6}$$

On the other hand, such total nucleon number can also be given by directly n-times integrating a density of the space, f, which only depends on r:

$$n\iiint f(r)r^2 sin(\theta)\,dr\,d\theta\,d\phi. \tag{7}$$

Hence, letting Eq. (6) be equal to Eq. (7), one can easily identify $f(r)$ as:

$$f(r) = \int \rho(r,\theta)sin(\theta)/2\,d\theta. \tag{8}$$

Namely, integrating $\rho(r,\theta)sin(\theta)/2$ over $[0,\pi]$ will give the nucleon density as a function of r, as shown in Fig. 1 (a).

In order to correctly reproduce the experimentally measured B(E2)↑ (Q_{20}) via Eqs. (4) and (5), one has to use the charge density distribution to represent the charge profile of the nucleus as realistically as possible. In this work, we assume that the charge density of nuclei can be calculated by folding the proton (neutron) density with the charge distribution of the proton (neutron):

$$\rho_{ch} = \int d^3r' [\rho_p(r') n_p(|r - r'|) + \rho_n(r') n_n(|r - r'|)], \tag{9}$$

where ρ_p (ρ_n) represents proton (neutron) density, while n_p (n_n) is the charge distribution of single proton (neutron). It's worth mentioning that the M-C Glauber simulation for the collision of two nuclei does not typically distinguish neutrons and protons, so we assume both neutrons and protons follow the same Woods–Saxon distribution in the form of Eq. (2) for simplicity, however, with different normalization factors:

$$\rho_p = \frac{Z}{A}\rho, \quad \rho_n = \frac{N}{A}\rho, \tag{10}$$

where Z, N and A denote proton number, neutron number and nucleon number, respectively. Based on this assumption, one can utilize B(E2)↑ (Q_{20}) as a reference to optimize the Woods–Saxon parameters and then apply them to generate nuclei via a M-C simulation.

Often, in Eq. (2), all nucleons are considered as point-like, viz. n_p and n_n in Eq. (9) are described by delta functions. In a realistic case however, the finite size of the nucleon should be taken into account [19–21]. For protons, we adopt the experimentally supported dipole form of the charge profile [22], which reads:

$$n_p(r) = \frac{m^3}{8\pi} e^{-mr}, \tag{11}$$

with $m = \sqrt{12}/0.877$ reproducing the proton RMS-radius 0.877 fm. For neutrons, we use the following form [23]:

$$n_n(r) = -\frac{2}{3}\frac{\langle r_n^2\rangle}{r_1^2(r_1\sqrt{\pi})^3}\left(\frac{r}{r_1}\right)^2\left[1 - \frac{2}{5}\left(\frac{r}{r_1}\right)^2\right]e^{-(r/r1)^2}, \tag{12}$$

with $\langle r_n^2\rangle = -0.113$ fm^2 and $r_1 = \sqrt{2/5}\cdot 0.71$ fm. B(E2)↑ (Q_{20}) can then be obtained by using the above equations. However, our calculation shows that the contribution to Q_{20} from neutrons is very small (much less than 1%), so we neglect the charge form factor of neutrons and only take protons into account. In this case, Eq. (9) can be simplified to:

$$\rho'(r,\theta) = 2\pi \int_0^\infty dr' r'^2 \rho(r',\theta) \int_{-1}^{1} dz n(\sqrt{r'^2 + r^2 - 2rr'z}), \tag{13}$$

where r' represents the distance from the center of the nucleus (coordinate origin) to any possible charge points in the proton, while r represents the distance to the center of the proton. After integrating Eq. (13) numerically and employing Eq. (8), an integrated charge distribution of deformed nuclei that only depends on r can be obtained.

In the steps above, directly adopting parameters from e-A scattering is no longer valid. Fig. 1 (b) shows the charge density distribution of uranium and gold nuclei with a point-like and a finite-size profile. The same parameters of R_0 and a from Ref. [16] are taken for both profiles for each nucleus. Deviations between the two profiles can be seen from this figure implying the parameter sets for finite-size profiles need to be adjusted. A relatively larger radius R_0 and a smaller diffuseness a for the finite-size scenario is needed to reproduce the Woods–Saxon distribution inferred from electron scattering measurements.

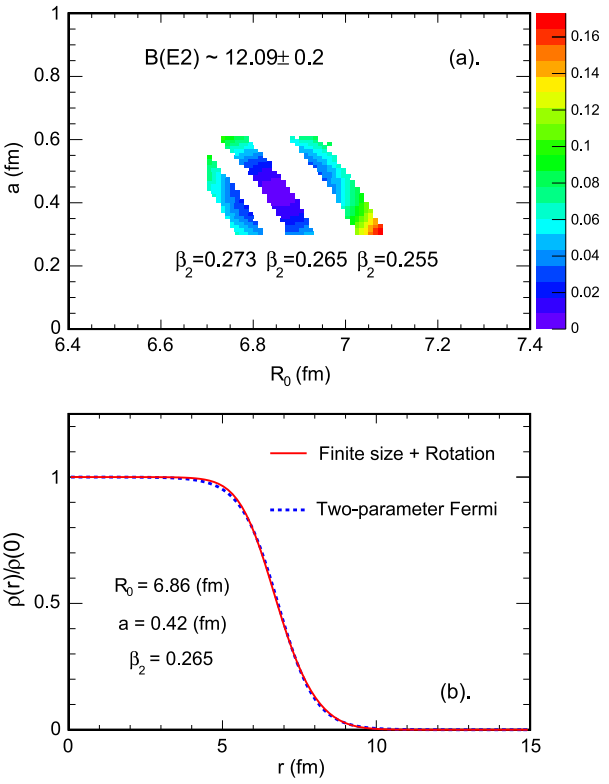

Fig. 2. (a) Two dimensional scan of R_0 and a for ^{238}U within the limit of B(E2)↑ error. Colors (z axis) represent different *SSR* values. The minimum *SSR* (purple) can be clearly seen at the center of colored region. (b) The experimentally measured charge distribution (two-parameter Fermi model) has been reproduced by Eq. (2) with the optimal parameter set. Here the B(E2)↑ value is 12.09. (For interpretation of the references to color in this figure legend, the reader is referred to the web version of this article.)

Now taking into account the finite size of nucleons and the presence of a deformation β_2, we want to find the set of parameters β_2, a, and R_0 that when used in Eq. (2) will yield a nucleus consistent with data on B(E2)↑ and electron scattering. During the implementation, we loop over all possible combinations of R_0, a and β_2. For each set, the deformed Woods–Saxon function with finite size profile is first rotated and then averaged. After that, the charge distribution with respect to the radius is extracted. Meanwhile, Q_{20} is directly calculated from Eqs. (4) and (13) in order to check for consistency with B(E2)↑. An optimal set should guarantee that (i) the charge distribution from electron scattering data is reproduced, (ii) the B(E2)↑ (Q_{20}) value from experiments can be obtained. For the first criterion, the sum of squares of the residual (*SSR*) is used to quantify the difference between the two distributions. In this work, only parameter sets providing minimum *SSR* and the nearest B(E2)↑ (Q_{20}) are considered in the final answer. We didn't tune β_4 because with its typical value, including β_4 makes little difference to our result.

3. Results

Fig. 2 shows an example of scanning optimal parameter sets for ^{238}U. According to Ref. [6], the B(E2)↑ value of ^{238}U is 12.09 ± 0.2 (e^2b^2). Within this experimental uncertainty, we calculate all possible combinations of R_0, a and β_2 to find the minimum *SSR*. Fig. 2 (a) shows the two dimension scan of the parameter sets. The anti-correlation between a and R_0 is due to the requirement that the

Table 1
Parameter sets for different nuclear species. The parameters listed in the "New" column are the parameters that take into account the finite size of nucleons and the deformation of the nucleus. "Old" parameters are taken from [6,16].

Nucleus	B(E2)↑	Par.	Old	New
^{238}U	12.09	R_0 (fm)	6.8054	6.86
		a (fm)	0.605	0.42
		β_2	0.2863	0.265
^{208}Pb	–	R_0 (fm)	6.62	6.66
		a (fm)	0.546	0.45
		β_2	0	0
^{197}Au	–	R_0 (fm)	6.38	6.42
		a (fm)	0.535	0.41
		β_2	–	−0.13

calculated B(E2)↑ from this procedure has to match previous measurement of B(E2)↑, of which the uncertainty is reflected as finite band width in the plot. The minimum SSR value visible in the plot corresponds to the purple region centered around the best parameters $R_0 = 6.86$ fm and $a = 0.42$ fm. The corresponding β_2 value that gives a nucleus with a Q_{20} consistent with the B(E2)↑ is 0.265. Fig. 2 (b) shows that the Woods–Saxon distribution is recreated by the above parameters with nice consistency with the one extracted from electron scattering. We summarize the parameter sets for different nuclear species in Table 1. For ^{208}Pb, the ground state nucleus is considered spherical [6] although its excited state may show a deformed configuration, thus the $\beta_2(^{208}\text{Pb})$ is taken to be 0 in this study. Namely, the only contributing step for ^{208}Pb in the aforementioned procedure is the finite-size correction. For ^{197}Au, B(E2)↑ has not been reported from experiments, therefore β_2 remains a major uncertainty in the initial conditions for Au + Au collisions. Therefore we fix the commonly used value $\beta_2(^{197}\text{Au}) = -0.13$, which comes from a mix of data and model calculations [24], and only provide the updated R_0 and a values with the caveat that these values will change if the β_2 is changed.

4. Eccentricity

To test how the corrections to the Woods–Saxon parameters may affect observables, we study the multiplicity distribution, the second and third harmonic participant eccentricity (ε_2 and ε_3) in U + U collisions from a Glauber model similar to the one discussed in Ref. [25] with parameters from Ref. [16] and Table 1. To generate the multiplicity, we use a two-component model. First define

$$n_{AA} = (1 - x_{hard})N_{part}/2 + x_{hard}N_{bin}, \tag{14}$$

where N_{part} is the number of struck nucleons, N_{bin} is the number of binary nucleon–nucleon collisions, and x_{hard} is a fractional contribution of N_{bin} to the multiplicity [15,26]. The multiplicity is then generated by sampling a negative binomial distribution n_{AA} times with negative binomial parameters (n_{pp} and k) taken from p + p collisions at the same energy and in the same $|\eta|$ window [27]. For this calculation we use the parameters $n_{pp} = 2.43$ and $k = 2$ for the negative binomial and $x_{hard} = 0.13$.

Fig. 3 shows the $dN/d\eta$ distributions in U + U collisions at $\sqrt{s_{NN}} = 193$ GeV from our Monte Carlo Glauber model calculations. The maximum $dN/d\eta$ with the new parameters is slightly higher than that with the original parameters. The increase comes from the smaller skin depth in the new parameters. As the skin depth becomes larger, the nucleus becomes more diffuse leading to a smaller N_{bin} and smaller estimate for $dN/d\eta$.

To study the impact of the new Woods–Saxon parameters on the initial geometry, we calculate the second and third harmonic participant eccentricity. Since different input parameters generate different multiplicity distributions, we present the eccentricities as

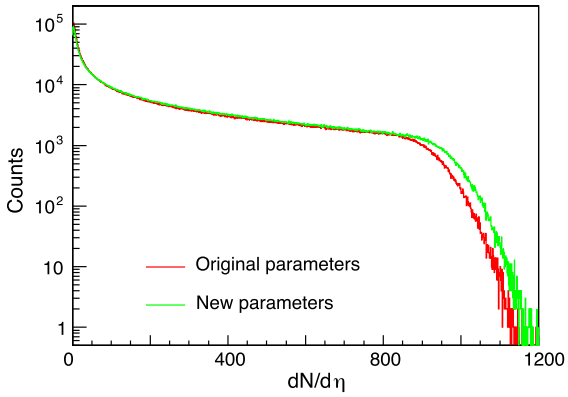

Fig. 3. (Color online.) The $dN/d\eta$ distributions in U + U collisions at $\sqrt{s_{NN}} = 193$ GeV. Two different sets of input parameters are compared.

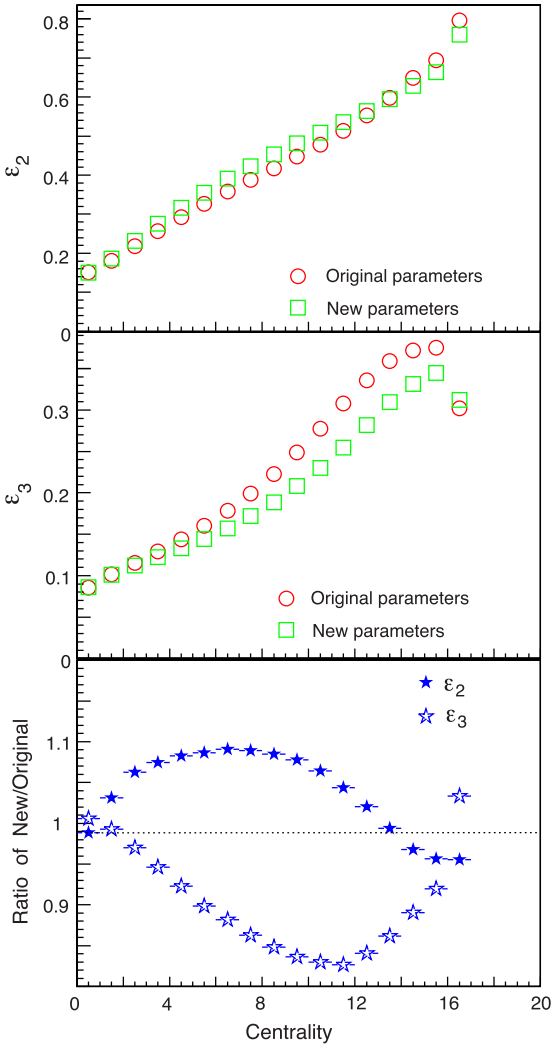

Fig. 4. (Color online.) The second and third order participant plane eccentricity as a function of centrality bins from Glauber model calculations. Centrality bins 0 to 20 represent the centrality range 0 to 100% in 5% increments with bin 1 corresponding to 0–5%.

a function of centrality intervals based on the percentage of the total multiplicity. In Fig. 4 upper and middle panels show ε_2 and ε_3 for the two parameters sets. The lower panel shows the ratio of the results with the parameters over the results with old parameters for ε_2 and ε_3. For the most central collisions, both ε_2 and ε_3 ratios are below one. For the most central bin, the initial geometry is

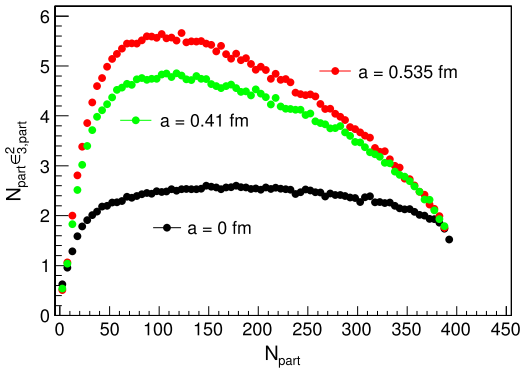

Fig. 5. Glauber model results for $N_{part}\varepsilon_3^2$ vs N_{part} for three cases: a diffuse nucleus $a = 0.41$ fm (new parameters), $a = 0.535$ (old parameters), or a hard sphere nucleus $a = 0$ fm. (For interpretation of the references to color in this figure legend, the reader is referred to the web version of this article.)

most sensitive to β_2 so the smaller β_2 values in the new parameter set lead to a smaller ε_2 and ε_3. In mid-central collisions, however, the new parameter set produces larger ε_2 values but smaller ε_3 values. This behavior can be traced to the smaller value of a in the new parameter set. In non-central collisions, the value of ϵ_3 is enhanced by the probability of a nucleon fluctuating out on the edge of one nucleus and impinging on the center of the other nucleus where it encounters a relatively large number of nucleons. This effect will be largest when the nucleon from nucleus A fluctuates in the reaction plane towards nucleus B. That configuration enhances ε_3 but decreases ε_2. It is this effect that explains the rise and fall of the ridge correlation in heavy ion collisions [13] and it also causes a correlation between the second and third harmonic event planes [28]. To further confirm this explanation, in Fig. 5 we show a Glauber model calculation of $N_{part}\varepsilon_3^2$ vs N_{part} for Au + Au collisions with a equal to 0.41 fm (diffuse, new parameter), 0.535 fm (diffuse, old parameter) and 0 fm (hard-sphere). For mid-central collisions with $N_{part} \approx 100$, the effect of the diffuseness amplifies ε_3 by a factor of nearly 2.1 (2.5) for new (old) parameters.

From this study, it is clear that the centrality dependence of ε_3 is strongly dependent on the diffuseness. For that reason, using the correct value of the diffuseness parameter when modeling heavy ion collision is crucial especially when calculating $v_3 = \langle\cos(3\phi)\rangle$ where ϕ is the azimuth angle of each particle relative to the major axis of the third harmonic event anisotropy. Since the relationship of v_3 and v_2 similarly defined are often used to estimate the viscosity to entropy ratio η/s, estimates of η/s from model-to-data comparisons can be adversely affected if the model does not use the correct Woods–Saxon parameters.

5. Summary

We find that when modeling the density distribution of deformed nuclei with a Woods–Saxon distribution, the radius R_0 and skin depth a used in the model will be substantially different than the average radius R_0' and skin depth a' that would be observed in electron scattering experiments. The more deformed the nucleus, the larger the discrepancy. For this reason, one must modify the parameters used in the Woods–Saxon model so that after appropriately averaging over all orientations of the axis-of-symmetry for the nucleus, the average radius R_0' and skin depth a' match the values reported from electron scattering experiments. In addition, one should also take into account the radius of the nucleon when carrying out a Monte-Carlo simulation of the positions of nucleons inside the nucleus, otherwise, the effective radius will be larger than the simulated radius by roughly the size of the nucleon. We also find that the model dependent β_2 parameters estimated from B(E2)↑ measurements, lead to an overestimate of the deformation of nuclei when they are used in a deformed Woods–Saxon distribution. We presented a procedure to calculate the correct values of the Woods–Saxon distribution for deformed nuclei (R_0, a, and β_2) so that the resulting nucleus is consistent with electron scattering data and B(E2)↑ measurements. Our calculations show that, for ^{238}U, ^{208}Pb and ^{197}Au, the new value of R_0 is slightly larger than the old value while the new value of a is significantly smaller. For ^{238}U, the obtained β_2 is also different than the ones that are commonly used. We also presented the results from Glauber-Model Calculations for U + U collisions to study the effect of the new parameters. The decrease in the skin depth has a large impact on eccentricity, increasing ε_2 but decreasing ε_3. Since the amount of viscous damping needed for a model to match v_3/v_2 data will depend strongly on $\varepsilon_3/\varepsilon_2$, overestimates of a will lead to overestimates of η/s. Predictions of models using the old parameter values may need to be revisited [29].

Acknowledgements

We would like to thank Thomas Ullrich and Ulrich Heinz for discussions and suggestions that lead to the initiation of this study. We thank Thomas Ullrich for the comments on the paper draft. A.H. Tang thanks G. Wang for discussion on one of the integrals. This work was partially supported by the U.S. Department of Energy under contract DE-AC02-98-CH10886, the Major State Basic Research Development Program in China under Contract No. 2014CB845401, the National Natural Science Foundation of China under contract Nos. 11421505, 11035009 and 11220101005, the Key Laboratory of Quark and Lepton Physics (MOE) and Institute of Particle Physics, Central China Normal University under contract Grant No. QLPL2015P02.

References

[1] J.-Y. Ollitrault, Phys. Rev. D 46 (1992) 229.
[2] K.H. Ackermann, et al., STAR Collaboration, Phys. Rev. Lett. 86 (2001) 402;
J. Adams, et al., STAR Collaboration, Phys. Rev. Lett. 92 (2004) 052302.
[3] J. Adams, et al., STAR Collaboration, Nucl. Phys. A 757 (2005) 102;
K. Adcox, et al., PHENIX Collaboration, Nucl. Phys. A 757 (2005) 184;
B.B. Back, et al., PHOBOS Collaboration, Nucl. Phys. A 757 (2005) 28;
I. Arsene, et al., BRAHMS Collaboration, Nucl. Phys. A 757 (2005) 1.
[4] D. Teaney, Phys. Rev. C 68 (2003) 034913.
[5] T. Hirano, U. Heinz, D. Kharzeev, R. Lacey, Y. Nara, Phys. Lett. B 636 (2006) 299.
[6] S. Raman, C.W. Nestor Jr., P. Tikkanen, At. Data Nucl. Data Tables 78 (2001) 1.
[7] U. Heinz, A. Kuhlman, Phys. Rev. Lett. 94 (2005) 132301;
A. Kuhlman, U. Heinz, Phys. Rev. C 72 (2005) 037901;
A. Kuhlman, U. Heinz, Y.V. Kovchegov, Phys. Lett. B 638 (2006) 171;
C. Nepali, G. Fai, D. Keane, Phys. Rev. C 73 (2006) 034911.
[8] L. Adamczyk, et al., STAR Collaboration, arXiv:1505.07812 [nucl-ex], 2015.
[9] M. Miller, R. Snellings, arXiv:nucl-ex/0312008, 2003.
[10] B. Alver, B.B. Back, M.D. Baker, et al., Phys. Rev. C 77 (2008) 014906.
[11] R.S. Bhalerao, J.-Y. Ollitrault, Phys. Lett. B 641 (2006) 260.
[12] W. Broniowski, P. Bożek, M. Rybczyński, Phys. Rev. C 76 (2007) 054905.
[13] P. Sorensen, J. Phys. G, Nucl. Part. Phys. 37 (2010) 094011;
P. Sorensen, B. Bolliet, Á. Mócsy, Y. Pandit, N. Pruthi, Phys. Lett. B 705 (2011) 71.
[14] G. Agakishiev, et al., STAR Collaboration, Phys. Rev. C 86 (2012) 014904.
[15] M.L. Miller, K. Reygers, S.J. Sanders, P. Steinberg, Annu. Rev. Nucl. Part. Sci. 57 (2007) 205.
[16] H. De Vries, C.W. De Jager, C. De Vries, At. Data Nucl. Data Tables 36 (1987) 495.
[17] P. Filip, R. Lednicky, H. Masui, N. Xu, Phys. Rev. C 80 (2009) 054903.
[18] F. Villars, in: C. Bloch (Ed.), Proceedings of the International School of Physics "Enrico Fermi" Course XXXVI, Many Body Description of Nuclear Structure and Reactions, Varenna on Lake Corno, 1966, Academic, New York, 1965, p. 31.
[19] T. Hirano, Y. Nara, Phys. Rev. C 79 (2009) 064904.
[20] W. Broniowski, M. Rybczyński, P. Bożek, Comput. Phys. Commun. 180 (2009) 69.
[21] M. Rybczyński, G. Stefanek, W. Broniowski, P. Bożek, Comput. Phys. Commun. 185 (2014) 1759–1772.
[22] F. Borkowski, G.G. Simon, V.H. Walther, R.D. Wendling, Z. Phys. A 275 (1975) 29–31.
[23] S. Haddad, S. Suleiman, Acta Phys. Pol. B 30 (1999) 119.

[24] P. Moller, J.R. Nix, W.D. Myers, W.J. Swiatecki, At. Data Nucl. Data Tables 59 (1995) 185;
W.M. Itano, Phys. Rev. A 73 (2006) 022510;
C. Nair, M. Erhard, A.R. Junghans, et al., Phys. Rev. C 78 (2008) 055802.
[25] H. Masui, B. Mohanty, N. Xu, Phys. Lett. B 679 (2009) 440.
[26] D. Kharzeev, M. Nardi, Phys. Lett. B 507 (2001) 121.
[27] R.E. Ansorge, UA 5 Collaboration, Z. Phys. C, Part. Fields 43 (1989) 357.
[28] D. Teaney, L. Yan, Phys. Rev. C 83 (2011) 064904.
[29] B. Schenke, P. Tribedy, R. Venugopalan, Phys. Rev. C 86 (2012) 034908;
B. Schenke, P. Tribedy, R. Venugopalan, arXiv:1403.2232 [nucl-th], 2014.